

OMAE2010-2\$,) +

LOW COST INERTIAL MEASUREMENT UNIT APPLICATION ON SUB-SEA LAUNCHING – SIGNAL PROCESSING AND TRAJECTORY ALGORITHM

Rodrigo Sauri Lavieri
University of São Paulo
São Paulo, SP, Brazil

Eduardo Aoun Tannuri
University of São Paulo
São Paulo, SP, Brazil

André L.C. Fajarra
University of São Paulo
São Paulo, SP, Brazil

Celso P. Pesce
University of São Paulo
São Paulo, SP, Brazil

Diego Cascelli Corrêa
PETROBRAS E&P
Naval Engineering
Rio de Janeiro, RJ, Brazil

ABSTRACT

Many situations in the Offshore Industry require equipment to be launched to the sea floor, becoming important to measure or to estimate their final position and/or to determine the complete trajectory. Some examples are the installation of anchorage devices, manifolds or production line supports. The main problem associated with the estimation of the position and the trajectory of the equipment is related to the fact that, systems such as GPSs and magnetometers cannot be used in subsea conditions. Gyrocompass and precise inertial sensors can be used, but they are expensive equipments and there is the risk of damaging during the launch process. The solution is to develop cost-effective inertial positioning systems that reach the operational requirements related to measuring accuracy. These equipments are based on MEMS (Micro-Electrical Mechanical Systems) inertial sensors that are relatively cheap. However, without the proper care, the signals obtained by these equipments present large levels of noise, bias and poor repeatability.

The aim is to show a sequence of test procedures, treatment and processing of signals that leads one to know the position, attitude and trajectory of a submarine device. Furthermore, it allows the quantification of errors and, eventually, their sources. A commercial IMU (Inertial Measurement Unit) was chosen as a case study. It is equipped with MEMS sensors, usually adopted by the automobile industry.

Tests with IMU were carried out intending to find the sensors scale factors, their bias and temperature sensitivity. Thereafter, the data were processed by two distinct algorithms. The first one is a simple algorithm that computes the attitude, azimuth at the final position and calculates the terminal velocity during the launch. The second one integrates the signal along

all the movement by using quaternions algebra, resulting in the complete trajectory of the body. Discussions about the accuracy, applicability and limitations of each method are presented.

INTRODUCTION

The two main kinds of sub-sea launching procedures in offshore industry are vertical or pendulous. The first case is represented by deep water anchor deployment, while the second case covers mainly positioning of manifolds. This work focuses on vertical launching. Although this case seems to be simple from kinematics point of view, it brings a great challenge to precisely determine the final attitude of the body, since it is, usually, buried underneath the sea floor. An IMU (Inertial Measurement Unit) is usually employed to register the fall's maximum velocity and the final body's attitude.

Albeit supported by inertial navigation theory, the purpose is to appoint the final position of a certain body on the sea floor. It is not in the scope of this work to do any real time integration or design a control system. It is assumed that the signal is already known, i.e. the IMU launched with the system has already been recovered and the data downloaded.

NOMENCLATURE

$\alpha_{X,Y,Z}$	Accelerometer X,Y,Z signal (acceleration in body frame)
θ	Inclination Angle (from the vertical)
ψ	Spin angle (Euler's description)
ϕ	Precession angle (Euler's description)
g	Gravity acceleration (scalar)

ACQUISITION AND SIGNAL TREATMENT

As mentioned before, the IMU utilized to monitor the launching of the system has to be relatively cheap since there is the risk of losing or damaging it. High-end IMUs have most of their cost related to the sensors they carry. To reduce IMU cost it is necessary to apply cheaper sensors. The cheapest sensors nowadays are MEMS (Micro-Electro-Mechanical Systems). As can be seen from Table 1, regular MEMS based on accelerometers and rategyros have prices 100 to 1000 times lower than precision inertial sensors.

Table 1-Comparison between motion sensors

Sensor	Brand	Based	Approx. Price [US\$]
Accele.	Analog Devices	MEMS	8.13
Accele.	Honeywell	Piezoelectric	310.00
Gyro	Analog Devices	MEMS	20.98
Gyro	Vibtel	FOG	12,000.00

The prices in Table 1 refer to the sensors, not to the ensemble IMU. One can deduce that MEMS based IMU can cost from two to ten times less than those which apply high end sensors.

Unsurprisingly, the reduced price implies the degradation of the signal quality. At this point it is interesting to define “signal quality” from the inertial navigation perspective. Reference [1] brings in detail many error sources of inertial sensors such as: nonlinearity, asymmetry or tilt misalignment. Among all these sources only few are relevant to our application. The sensor quality is greatly related to the non deterministic errors of its output signal due to the fact that the deterministic ones, once measured, can be, somehow, removed from the signal.

The principal deterministic error observed in the study case was the bias stability. The bias is the sensor reading when there is no input signal on it. It is a “constant” value added to the signal and, therefore it can be easily subtracted from it. The bias stability ensures that it is actually constant during acquisition time.

Bias is especially important when the output signal must be integrated. Even minimum drifts can cause great position errors due to the integration process. Acceleration bias causes error which grows in a quadratic relation with the time while rate bias produces an attitude error that grows linearly.

A common method to evaluate bias stability is to calculate the Allan variance of the signal. A better description of the method can be found in [2] but, in general, it allows one to verify the variance calculated from different sizes of intervals taken from the whole signal.

According to [2] the bias stability is represented by the lowest point of the variance curve. According to Figure 1, showing the Allan variance, it is possible to see that the applied rategyros have bias stability near 0.01deg/s, different to fiber optical based gyros which present this value around 0.5deg/h (1.4×10^{-4} deg/s).

The slope in the initial part of the curve, before it reaches the lowest point, is directly correlated to the sensor noise [2]. It is easy to check because a simple moving average filter can make Allan variances’s curve much more horizontal.

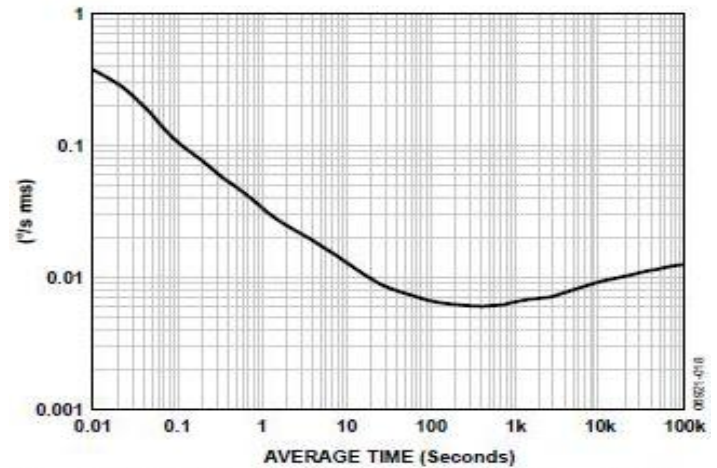


Figure 1-Rategyro's Allan Variance (from manufacturer)

Previous launching operations showed that the acquisition time is between 15 and 60s and it matches the interval where the bias stability value is well determined.

MEMS sensors are considerably affected by changes in environment temperature. MEMS accelerometers and rategyros are composed by small beams used to measure the forces. The stiffness of those beams can change substantially with temperature, resulting in measurement drift. Modeling this dependence has been the object of several studies such as [4] for instance; it highlights the hysteresis present in great temperature changes.

Sensors' manufacturers usually provide experimental data from limits of the working temperature range. It leads to a linear approximation that, in some cases, does not help enough. The best thing to do is to test all the sensors in a climate chamber and establish specific correction models. Most of the corrections of bias drift due to temperature made in this project, using data from manufacturer, were unsuccessful.

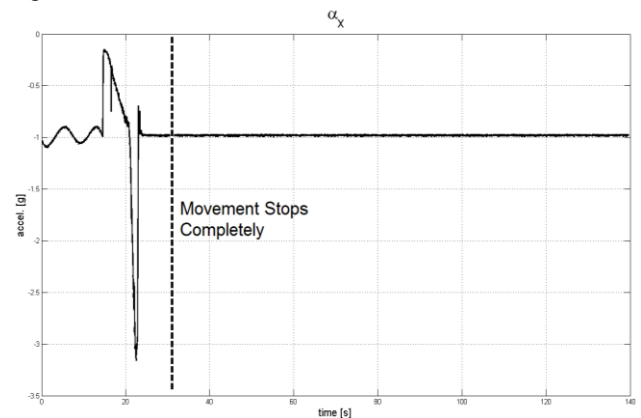


Figure 2-Point where movement extinguishes

The solution found was to calculate bias directly from the acquired signal. For rate data, it can be done directly because it is known that enough time after the impact with the ocean floor, the IMU unit will be motionless and the gyros reading should be null as shown in Figure 2.

After the fall, the IMU will most likely have an angle with the vertical. It will cause a non-null reading in each accelerometer caused by gravity projection. In order to estimate the bias in this case it is necessary to do a coordinate frame transformation and the gravity correction. This procedure will be detailed later in this text.

Another important calibration parameter is the scale factor of the sensor. In most analogical sensors, it is given in g/V or deg/s/V. In the present case it is a non-dimension value since the IMU that has been used is a commercial version – black box - device and provides pre-treated measurements.

The scale Factor is the slope of the line that correlates sensor input and output. This parameter is usually given by the sensor manufacturer but it is important to verify its accuracy. The non linearity of the signal is another important parameter of the sensor, and it is also provided in the sensor specification sheet. Even the cheaper sensor presents good linearity, in other words, the non-linearity keeps under 0.1% of full length scale.

In order to verify the scale factor of the sensors used in this work, bench tests were performed involving a tilt vise and a rate table.

The accelerometer scale factor was determined using a tilt clamp as can be seen in Figure 3(a). The input signal was the gravity acceleration perceived by the pair of accelerometers aligned with the vertical plane where the inclination took place. The expected measurement, in g's, would be given by the following expressions

$$\alpha_x \text{ expected} = \cos(\theta) \quad (1)$$

$$\alpha_y \text{ expected} = \sin(\theta) \quad (2)$$

$$\alpha_z \text{ expected} = \sin(\theta) \quad (3)$$



Figure 3 - (left) Experimental assembly (right) Inclinometer position

The tilt angle was measured using the clamp scale and an inclinometer (Mitutoyo Pro 360) fixed together with the IMU (Figure 3(b)).

After these experiments, it was possible to create the input x output graphs for accelerometers in each axe of the IMU. Figure 4 shows the signal of accelerometer X for each expected reading related to the inclination angle. Each point corresponds to the average of a 10s acquisition and they are distributed in clusters because, in every inclination angle, 10 acquisition were made.

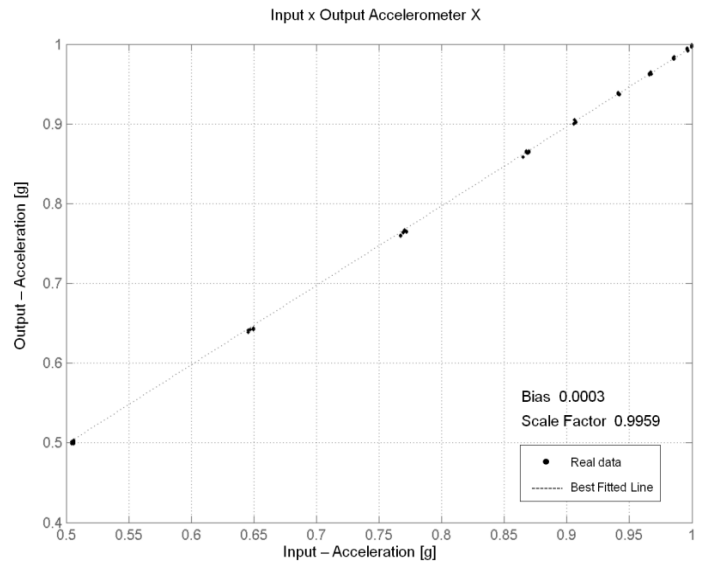


Figure 4-Input x Output of Accelerometer X (calibration curve)



Figure 5-Rate table assembly

The straight line in Figure 4 was fitted by the least square method of the data and the linear coefficient and the angular

coefficient are shown as Bias and Scale Factor respectively in the graph. As indicated by the bias and scale factor shown in the graph, the accelerometers are well calibrated.

That one may determine the rategyros scale factors necessary to use a rate table. It is a device equipped with a rotating platform where the IMU or a single sensor is fixed (Figure 5) and it is possible to apply precisely known angular velocities.

Once the IMU was fixed with the sensor sensitive axe aligned to the table rotating axis, a constant angular velocity was applied. The sensor acquisition was started only after the rate table had reached a constant speed; it made the signal constant during the experiment. Each signal, just as in the inclination experiment, had its mean calculated and the whole data was compared in Figure 6.

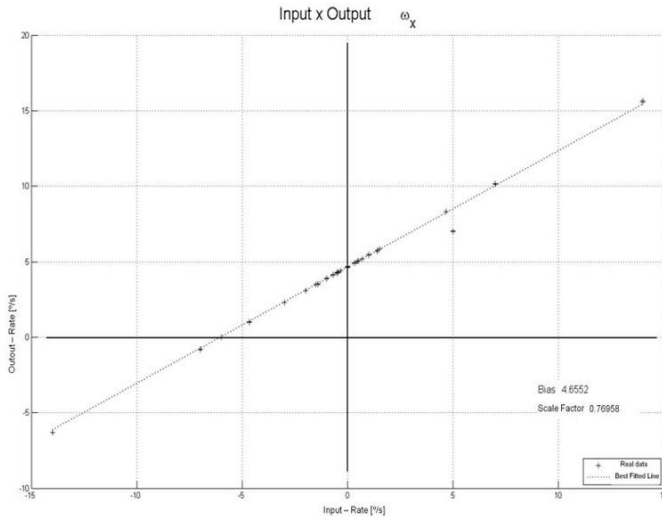


Figure 6- Input x Output of Rategyro X

The X axis –axis pointing downward before the launching–represents the input rate, guaranteed by the rate table precision –it is an Ideal Aerosmith 1291BR– and the Y axes correspond to the output signal in deg/s. Following the same steps performed for the acceleration data, a straight line was fitted and the bias and scale factor obtained from its coefficients. In the example shown in Figure 6 neither linear coefficient nor angular coefficient were well calibrated.

TRAJECTORY RECONSTRUCTION ALGORITHM

The main information on the trajectory in the case of the launch of an anchorage device are: the maximum speed reached during the fall, the final inclination and its azimuth. The azimuth angle can be defined as the angle between the vertical plane containing the entire body - the same divide symmetrically- and a vertical reference plane.

Algorithm I- geometric

The first approach proposed does not require the reconstruction of the whole trajectory. The calculations are focused on determining the elements described above. In order to do that some hypothesis were made, the main one being that

the body falls following a vertical trajectory. Considering this hypothesis and the information that the X accelerometer sensitive axis is pointing downward, the final velocity is calculated as the time integral of α_x . Figure 7(a) shows the vertical velocity calculated without any bias correction while Figure 7(b) shows the same quantity with bias correction.

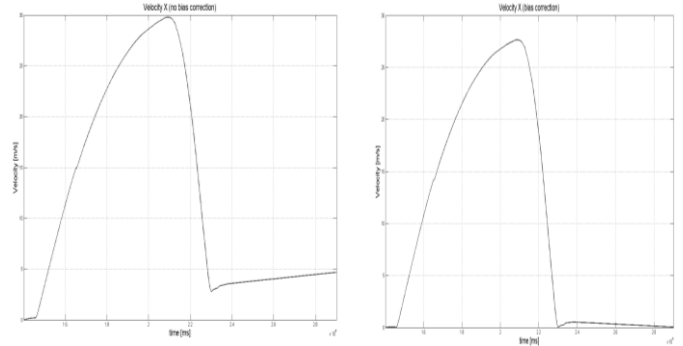


Figure 7- (left) Vertical Velocity without bias correction (right) Vertical Velocity after acceleration bias correction

This comparison exemplifies the correction procedure proposed earlier for the acceleration signal. Besides the bias error, the hypothesis that the trajectory is vertical also causes an additional drift proportional to $\cos(\theta)$.

The final inclination is calculated based on the reading of gravity in each axis of the IMU. It can be simply shown that the inclination is given by the equation (4).

$$\theta = \arctan \left(\frac{\sqrt{\alpha_y^2 + \alpha_z^2}}{\alpha_x} \right) \quad (4)$$

This equation holds whenever the only force acting on the body is gravity and it is vertical, or it represents the reference for angle measurement.

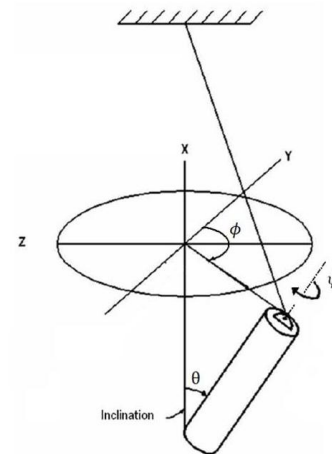


Figure 8-Euler's angles on anchorage system

The final azimuth information is less intuitive and more fraught with simplifying assumptions, according to this approach. The azimuth is calculated from three pieces of information: an initial angular condition, the integral of the angular velocity and a parcel spin – proper rotation - measured from the final condition acceleration resultant -equation(5)-. To detail this calculation, it is important to adopt the description of Euler angles (Figure 8).

$$Azimuth_{final} = Azimuth_{initial} + Azimuth_{rotation} + Azimuth_{bottom} \quad (5)$$

The initial condition must be known either by mechanical constraints or by visual inspection performed by a ROV.

The second part of the equation (5) involves the integration of the spin around the axis X, by the hypothesis of almost vertical motion as shown in equation (6) and (7). This integral is strongly affected by the signal errors, described in the previous section.

$$Azimuth_{rotation} = - \int (\dot{\psi} + \dot{\phi} \cos \theta) dt \quad (6)$$

Assuming small angles,

$$Azimuth_{rotation} = -(\psi + \phi) = \int \omega_x dt \quad (7)$$

This last statement is based on the fact that for small inclination angles, spin and precession blend. The last component of equation (5) is calculated by expression (8).

$$Azimuth_{bottom} = \arctan\left(\frac{\alpha_z}{\alpha_y}\right) \quad (8)$$

To better understand the last equation (8) one should see Figure 9. Finding the angle in which tangent represents the projection gravity acceleration vector on the body transversal plane –plane containing accelerometer y and z –, it is possible to find out where the longitudinal axe of the body is pointing to.

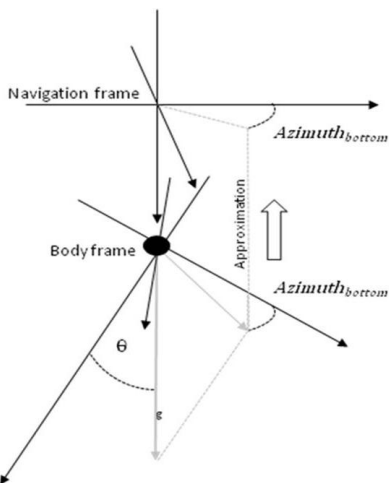


Figure 9 – Bottom azimuth prediction process and approximation made

As shown in the following formula, this term of the equation (5) is related to the body spin.

$$M = \begin{bmatrix} \cos(\psi + \phi) & -\sin(\psi + \phi) & \theta \cos(\phi) \\ \sin(\psi + \phi) & \cos(\psi + \phi) & \theta \sin(\phi) \\ -\theta \cos(\psi) & \theta \sin(\psi) & 1 \end{bmatrix} \quad (9)$$

M represents the rotation matrix with the simplifications of small angles. Also knowing that the body is motionless, the only accelerometers reading will be the gravity that, in body frame, is given by equation (10).

$$g = [M] \begin{bmatrix} 0 \\ 0 \\ g \end{bmatrix} = g \begin{bmatrix} -\theta \cos(\psi) \\ \theta \sin(\psi) \\ 1 \end{bmatrix} \quad (10)$$

Using this result in equation (8),

$$Azimuth_{bottom} = \arctan\left(\frac{-\cos(\psi)}{\sin(\psi)}\right) = \psi - \frac{\pi}{2} \quad (11)$$

Considering null initial condition, expression can be reinterpreted as:

$$Azimuth_{final} = -\left(\frac{\pi}{2} + \phi\right) \quad (12)$$

Equation (12) shows the azimuth aimed in this work using Euler's description.

Algorithm II– quaternion's

The second approach eliminates all the simplifying assumptions and is based on the integration of the signal throughout the whole launching motion. The IMU considered is the strapdown type [5], i.e. the sensors are attached to the body and there is a need to know their attitude at every instant in order to make the integration in the navigation frame.

The decision was to use quaternions instead of matrices of cosines directors (MDC) because the number of equations to be solved moment to moment is smaller - 4 for the quaternions and 9 for MDCs – the need to re-normalize the vectors from time to time is also reduced - the quaternion of rotation tends to keep its unitary length - and finally the integration using quaternions is free of gimbal lock - loss of one degree of freedom due to the alignment of two axes of rotation [5] -. For more information about spatial rotations using quaternions, reference [6] is suggested. The procedure is to calculate the attitude of the body at a given time executing a small rotation on the last integration step frame, then bring the accelerations at the body frame to the reference frame – navigation frame, discount the acceleration of gravity and advance with the integration. Although described in detail in reference [5], steps of the algorithm are summarized below:

$$q_{k+1} = \exp\left(\frac{\Sigma_k}{2}\right) q_k \quad (13)$$

where,

$$\Sigma_k = \int_{t_k}^{t_{k+1}} \begin{bmatrix} 0 & -\omega_x & -\omega_y & -\omega_z \\ \omega_x & 0 & \omega & -\omega_y \\ \omega_y & -\omega_z & 0 & \omega_x \\ \omega_z & \omega_y & -\omega_x & 0 \end{bmatrix} dt \quad (14)$$

Being able to calculate the quaternion of rotation for each instant of time the next step is to use them to bring the acceleration to the navigation frame. Equation (15) executes the transformation; likewise it calculates the velocity increment in the integration step \mathbf{u}_k^n .

$$\mathbf{u}_k^n = \mathbf{q}_k \cdot \left(\mathbf{v}_{k+1} + \frac{1}{2} \boldsymbol{\alpha}_{k+1} \times \mathbf{v}_{k+1} \right) \cdot \mathbf{q}_k^* \quad (15)$$

and,

$$\boldsymbol{\alpha}_{k+1} = \int_{t_k}^{t_{k+1}} \boldsymbol{\omega} dt \quad (16)$$

It is important to observe that the multiplication shown in equation (15) is a multiplication of quaternions [7]. Expression (17) brings the last step which is the effective integration of acceleration.

$$\mathbf{v}_{k+1}^n = \mathbf{v}_k^n + \mathbf{u}_k^n + \mathbf{g} dt \quad (17)$$

It can be seen in equation (17) that the gravity must be subtracted from the velocity. The signal of the gravity term depends on the orientation chosen at the beginning of the integration process.

The only simplifying assumption made in this case is that angular velocity $\boldsymbol{\omega}$ remains the same during the integration step. It is quite reasonable since the rates are low when compared to the acquisition rate of the sensors – 100Hz-.

In spite of the fewer simplifying hypothesis of this algorithm, it is more dependent on the signal errors. It happens because all parameters are calculated via integration and, as has been stated previously, bias produces great position errors when integrated over time. In fact, the signal quality is directly related to the time period in which this integration produces reasonable results.

In the case study, the time of the fall did not exceed 15 s and the results of trajectory reconstruction remained acceptable as will be seen.

For the purpose of comparison, Figure 10 shows the same quantity of Figure 7 but obtained from a distinct method.

As can be seen from Figure 11, the quaternion algorithm allows one to knowing the attitude of the body at every instant.

In terrestrial applications other sources of data are incorporated into the IMU, such as GPS or magnetometers. The position obtained from the integration of inertial sensors signals is compared with the position from the second source of

information through the Kalman filter. This information combination greatly improves the performance of the unit mainly by eliminating drift accumulated in the integration processes. In this work, however, the performance of the IMU alone is studied.

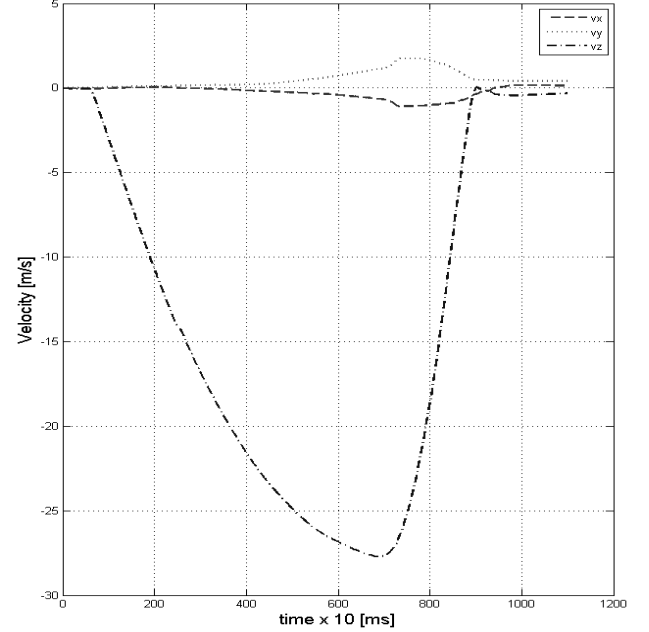


Figure 10-Velocities in navigation frame calculated using quaternion's

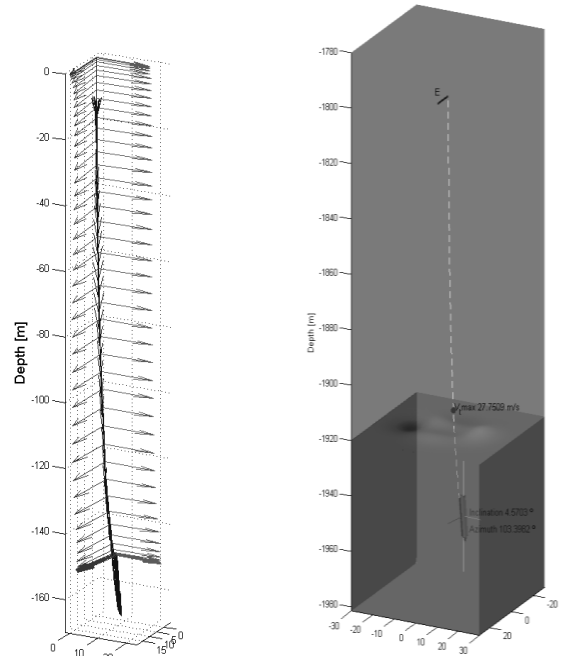


Figure 11 - (left) Body frame over time; (right) Pile's Trajectory

RESULTS COMPARISON AND CONCLUSIONS

This work demonstrated that by applying a simple signal correction the results from the geometric algorithm were closer than those obtained from the quaternion's approach. The final inclination from the first method came from the acceleration data -equation (4)- while the same quantity, in the other algorithm, was calculated by the integration of angular velocities. The same happened for the azimuth; one of the methods applied gravity acceleration while the other used inertial accelerations. The distinct character of the methods leading to a close result strengthens the premise that the signal correction is being conducted correctly and is getting the results closer to reality.

The procedure still presents important limitations such as the integration time. The results shown here were obtained for about 15s of integration. Table 2 displays the main results from the different approaches.

Table 2 – Final results

Algorithm I (no signal correction)			
Experiment	Max Velocity [m/s]	Final Inclination [°]	Final Azimuth [°]
1	29.78	4.4	23.5
2	28.35	5.2	268.1
3	29.79	6.4	122.8
Algorithm I (signal corrected)			
1	27.65	4.4	37.2
2	25.47	5.2	277.4
3	27.25	6.4	130.8
Algorithm II (signal corrected)			
1	27.75	4.6	41.9

2	25.49	4.9	280.8
3	27.18	6.4	127.7

ACKNOWLEDGMENTS

The authors acknowledge Petrobras for the financial support and for the motivation of this work. The first author acknowledges the Coordination for the Improvement of Higher Level -or Education- Personnel (CAPES) for the research grant.

EA Tannuri and CP Pesce acknowledge the National Council for Scientific and Technological Development (CNPq) for the research grants.

REFERENCES

1. LAWRENCE, A. **Modern Inertial Technology**. New York: Springer, 1998.
2. STOCKWELL, W. **Bias Stability Measurement: Allan Variance**. [S.l.]. 2004.
3. ANALOG DEVICES. **ADXRS613 datasheet**. Norwood. 2008.
4. GULMAMMANDOV, F. Analysis, Modeling and Compensation of Bias Drift in MEMS Inertial Sennsors. **4th International Conference on Recent Advances in Space Technologies** , 11-13 jun 2009.
5. TITTERTON, D. H.; WESTON, J. L. **Strapdown Inertial Navigation Technology**. Reston: AIAA, 2004.
6. DIEBEL, J. **Representing Attitude: Euler Angles, Unit Quaternions, and Rotation Vectors**. Stanford. 2006.
7. KUIPERS, J. B. **Quaternions and Rotation Sequences**. Princeton: Princeton University Press, 1999.